

# Characterization of a multilayer soft X-ray reflector fabricated by pulsed laser deposition

Dong-Eon Kim <sup>a,\*</sup>, Soo-Mi Lee <sup>a</sup>, In-Joon Jeon <sup>a</sup>, M. Yanagihara <sup>b</sup>

<sup>a</sup> Physics Department, Pohang University of Science and Technology, San 31 Hyoja-Dong, Pohang, Kyungbuk 790-784, South Korea

<sup>b</sup> Research Inst. of Scientific Measurement, Tohoku University, Sendai, Japan

---

## Abstract

A Mo/Si multilayer (ML) has been fabricated as a reflector in the soft X-ray spectral region by pulsed laser deposition (PLD), using the second harmonic of Nd/YAG pulsed laser (5 ns, 532 nm light). The ML structure was characterized by transmission electron microscopy (TEM), small-angle X-ray scattering (SAXS) and photoelectron spectroscopy for chemical analysis (ESCA). The near-normal incidence reflectivity in the spectral range of 14–17 nm was measured using a soft X-ray reflectometer based on a laser-produced plasma. The structural parameters were evaluated by fitting to both the SAXS profile and the soft X-ray reflectance measurement with asymmetric interface profile, roughness and composition taken into account. © 1998 Elsevier Science B.V.

PACS: 61.10.Lx; 68.55.Jk; 68.65.+g; 78.65.-s; 81.15.Jj

Keywords: Pulsed laser deposition; Multilayer; Soft X-ray reflectivity; Small-angle X-ray scattering

---

## 1. Introduction

Due to interface effect and the proximity of different materials, multilayer (ML) structures have unique properties different from bulks. One of the important applications of such unique properties is X-ray optics. A ML has an enhanced reflectivity at normal incidence and other useful properties for polarization, filter and dispersion in the soft X-ray spectral region and has been utilized to various soft X-ray instrumentations [1]: soft X-ray microscopes offering biologists a high-resolution imaging of spec-

imens in an aqueous state [2,3] and X-ray telescopes in astronomy [4]. Employing ML soft X-ray optics, the soft X-ray projection XUV lithography has demonstrated a resolution better than 0.1  $\mu\text{m}$  [5,6]. The need of ML soft X-ray optics is increasing as key elements in synchrotron beamline, for example, soft X-ray polarimeter [7].

Most of such ML X-ray optics have been successfully fabricated by magnetron sputtering or e-beam deposition. The deposition of metallic multilayer with pulsed laser deposition (PLD) has several advantages compared to other techniques. The pulsed nature of the process allows the control of layer thickness and growth rate by the number of laser pulses and the laser repetition rate, respectively. It is also possible to use virtually all metals as targets if a sufficient laser fluence is available. PLD is found to enable one

---

\* Corresponding author. Tel.: +82-562-279-2089; fax: +82-562-279-3099; e-mail: kimd@vision.postech.ac.kr.

to grow extremely thin metal films as thin as 0.5 nm [8]. Even though such advantages have made PLD applied to various areas of science and technology, it has not been much applied in the area of X-ray optics [9–11].

In this paper, we present our efforts of the fabrication of soft X-ray Mo/Si ML reflectors and their characterizations. A Mo/Si ML has been fabricated by PLD and characterized by small-angle X-ray scattering (SAXS) measurement at Cu  $K_{\alpha}$  transition and transmission electron microscopy (TEM) for structural analysis, electron spectroscopy for chemical analysis (ESCA) for compositional analysis, and soft X-ray reflectance measurement in the spectral range of 14–17 nm.

## 2. Fabrication of Mo/Si multilayer

The fabrication of a Mo/Si ML was performed on a HV device whose schematic diagram is shown in Fig. 1. This chamber was pumped down by a diffusion pump. Ar and other gases can be introduced into the chamber, depending on deposition conditions. For the ML under the present study, no gas was introduced and it was fabricated in low  $10^{-3}$

Torr. The target manipulation system can hold up to 4 targets with each target being self-rotating on its own axis and switch one target to another by rotation, as requested. The separation between a target and a substrate can be varied but the present Mo/Si ML was produced at 6 cm. The second harmonic of Nd/YAG pulsed laser (5 ns, 532 nm light) was used to ablate target materials. A lot of particulates are usually generated from Si target. The production of particulates was minimized by evaporating Si near threshold. This could not totally eliminate particulates but reduce their production greatly. A double pulse technique is currently under study. Two synchronized laser pulses (e.g., 532 and 532 nm lights, 532 and 266 nm lights) with a proper time delay are illuminated on a target. The first pulse is supposed to melt the target surface and the second pulse to ablate the melted material. Proper conditions such as the pulse time-separation and the energy of each pulse are under current study. The fluence of laser on targets was  $1.75 \text{ J/cm}^2$ . The deposition rate was calibrated using  $\alpha$ -step method to be 0.0091 nm/shot for Mo target and 0.017 nm/shot for Si target. The ML of 43 Mo/Si bilayers was deposited on a Si(100) wafer. The outmost top surface is Si in order to reduce the oxidation on surface.

## 3. Characterization

The structure of the Mo/Si ML was characterized by SAXS and TEM. The soft X-ray reflectivity at near-normal incidence ( $80^\circ$  from the surface) in the spectral region of 14–17 nm was also done using a soft X-ray reflectometer.

A conventional X-ray diffractometer was used to perform small-angle X-ray scattering experiments. It is equipped with a graphite crystal as a monochromator and delivers Cu  $K_{\alpha}$  radiation ( $\lambda = 0.154 \text{ nm}$ ). It provides an angular resolution of  $0.01^\circ$  and our  $\theta$ - $2\theta$  scan data shown in Fig. 2a were taken with an angular resolution of  $0.02^\circ$ .

Among the structural parameters such as the bilayer thickness,  $d$ , the thickness ratio of Mo layer to the bilayer thickness,  $\gamma$ , the interfacial diffusion,  $\sigma$ , the interfacial roughness,  $\Delta$ ,  $d$  and  $\gamma$  are the most important parameters to be determined first. They

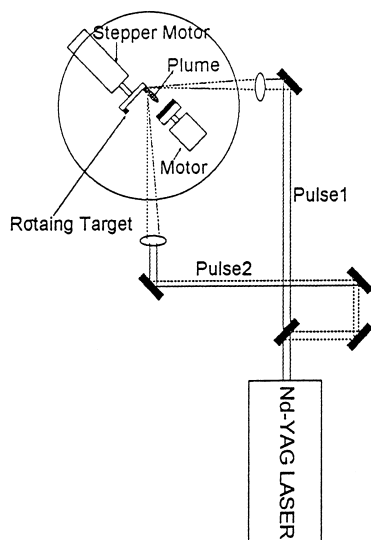


Fig. 1. Pulsed laser deposition system.

can be estimated [12] using the refraction-corrected equation for the Bragg condition:

$$\frac{m\lambda}{2 \sin \theta_m} = d_m = d \left( 1 - \frac{\delta}{\sin^2 \theta_m} \right), \quad (1)$$

where  $m$  is the order of Bragg peak,  $d_m$  the apparent period,  $d$  the average real period,  $\theta_m$  the angular position of the  $m$ th Bragg peak and  $1 - \delta = n$  the effective real part of the index of refraction of the ML structure. The apparent period,  $d_m$ , can be found from the angular positions of the Bragg peaks, and from the linear relationship between  $d_m$  and  $1/\sin^2\theta_m$ , the average real period of the multilayer structure,  $d$ , can be estimated. This is shown in Fig.

2(b) where  $d_m$  is plotted with respect to  $1/\sin^2\theta_m$ . The least-square fit yields  $d = 8.21$  nm with the standard deviation of 0.04 nm. From its slope, the decrement of the effective real part of the index of refraction of the ML structure can be evaluated, which can then be used to estimate  $\gamma$ , the ratio of the thickness of the Mo layer to the ML period:  $\gamma = (\delta - \delta_{\text{Si}})/(\delta_{\text{Mo}} - \delta_{\text{Si}})$ .  $\delta_{\text{Mo}}$  and  $\delta_{\text{Si}}$  are the decrements of the effective real part of the index of refraction of Mo and Si, respectively. These values are used as input values for the calculation of the SAXS patterns for comparison with experimental data.

To refine the bilayer thickness,  $d$ , and the thickness ratio,  $\gamma$ , and evaluate the interfacial diffusion,  $\sigma$ , the interfacial roughness,  $\Delta$ , the experimental SAXS data were fitted by computer calculation. The dynamical theory of X-ray scattering has been adapted in the recursive formalism [13]. The multiple reflections inside ML are taken into account. The detailed description of the computer code has been published [14–16]. The effect of such structural parameters on SAXS data has been previously studied [14–16]. The angular positions of the Bragg peaks are determined by the average bilayer thickness, the thickness ratio predominantly affects the shape of SAXS features in the small-angle region. Hence, the thickness ratio can be estimated by fitting the computer-generated SAXS pattern to the experimentally determined pattern in the small-angle region. Both interdiffusion and roughness decrease the intensities of the Bragg peaks. However, the broadening of the widths of the Bragg peaks is mainly due to uncorrelated roughness. This fact can be utilized for the estimation of roughness. The degree of interdiffusion can then be found by comparing the intensities of the Bragg peaks between the computer-generated and the experimental data with taking into account the reduction of the intensities due to roughness. Fig. 2a also shows the fit to the SAXS data. The reasonable agreement was obtained except in the area of the 4th Bragg peak and beyond. The parameters used to obtain this fit are  $d = 8.23$  nm,  $\gamma = 0.2$ ,  $\sigma_{\text{Mo-on-Si}} = 0.46$  nm,  $\sigma_{\text{Si-on-Mo}} = 0.2$  nm and  $\Delta = 0.6$  nm. The interface profile was assumed to be given by an error function. The compositional analysis by ESCA revealed the contamination by oxygen and carbon. The contamination by oxygen and carbon may be due to

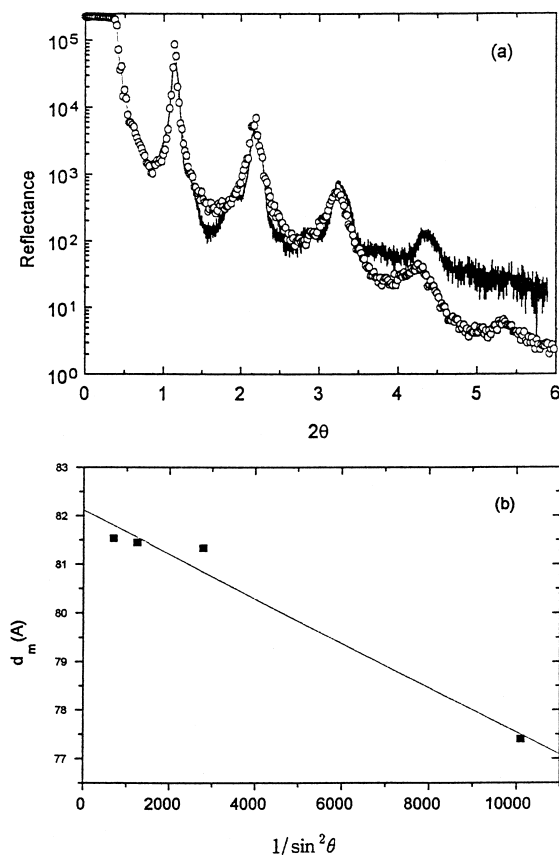


Fig. 2. (a) SAXS data and fitting by computer simulation. The structural parameters used for fitting are  $d = 8.23$  nm,  $\gamma = 0.2$ ,  $\sigma_{\text{Mo-on-Si}} = 0.46$  nm,  $\sigma_{\text{Si-on-Mo}} = 0.2$  nm and  $\Delta = 0.6$  nm. The contamination by oxygen (20% in number density) and carbon (41% in number density) is taken into account in the calculation. (b)  $d_m$  is plotted with respect to  $1/\sin^2\theta_m$  for the estimation of  $d$ .

the fabrication of our sample in low vacuum environment. Each layer contains about 41% of carbon and about 20% of oxygen. The contamination was taken into account in the calculation. This contamination has a slight effect on the SAXS profile due to little difference in optical constants between the elements at 0.154 nm but greatly reduces the reflectivity around 15.5 nm.

The soft X-ray reflectivity measurement was done using a soft X-ray reflectometer at Research Institute for Scientific Measurement, Tohoku University. It consists of a laser–target chamber, a concave collection mirror chamber, a monochromator, and a detection chamber [17]. A laser-produced plasma by a Q-switched Nd/YAG laser is used as a soft X-ray source. The monochromator can cover the spectral range from 9.5 to 31 nm with a samarium target. It uses a grating of 600 lines/mm and provides the resolving power of 240 at 25.6 nm with the exit slit width of 200  $\mu\text{m}$ . The measured near-normal-incidence reflectivity at 15.6 nm is about 1.2% as shown in Fig. 3. The calculation of reflectivity at 15.6 nm with the same structural parameters and composition as in the SAXS data analysis is also shown. There is a large difference in the magnitude of reflectivity. The difference between the calculation and the experimental data both in the reflectivity measurement and the SAXS (around the 4th Bragg peak) may be attributed to the wrong assumption for the interface

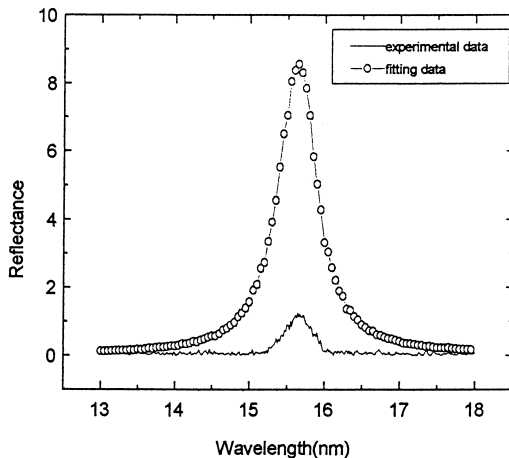


Fig. 3. Reflectivity measurement at the incidence angle of  $80^\circ$  in the spectral region from 14 to 17 nm. The calculation is also shown, which is done with the same structural parameters as used in Fig. 2a.

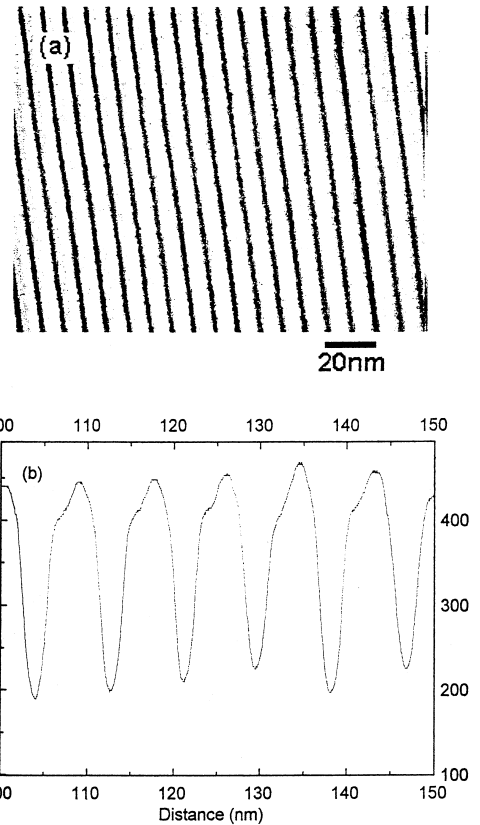


Fig. 4. (a) TEM micrograph, (b) densitometer scan.

profile. The TEM cross-sectional micrograph shown in Fig. 4 with its densitogram indicates not only a significant mixing (or transition layer) at each interface and asymmetric transition layers at the Mo-on-Si and Si-on-Mo interface but also a complicated density profile which can not be described by a simple error function. Further understanding requests the study of the effect of the density profile on the soft X-ray reflectivity, which is under investigation.

#### 4. Conclusion

The fabrication and characterization of a Mo/Si ML reflector in the spectral region of 14.0–17.0 nm have been described. The ML structure was deposited by PLD on a Si wafer in a relatively low vacuum. The ML reflector was examined by TEM, SAXS, ESCA and soft X-ray reflectivity measure-

ment. The TEM picture and the analysis of SAXS data indicate that there are asymmetric interdiffusion and roughness at each interface. The structural parameters were obtained from fitting to the SAXS data. TEM micrograph also reveals the complicated density profile which can not be prescribed by an error-function or exponential profile. The ESCA measurement indicates that the low-vacuum environment in deposition caused the significant contamination by carbon and oxygen. Such contamination and the complicated density profile may be attributed to the measured low reflectivity of about 1.2% at 15.6 nm at normal incidence.

### Acknowledgements

This work has been supported by the POSTECH/BSRI special fund 1996, the contract from Electronic Telecommunication Research Institute, the Basic Science Research Institute Program, Ministry of Education, 1996 (Project No. BSRI-96-2439), and Korea Science and Engineering Foundation (Project No. 96-0702-01-013).

### References

- [1] R.B. Hoover, A.N.C. Walker, Jr. (Eds.), *X-ray and Extreme Ultraviolet Optics*, Proc. SPIE 2515, 1995.

- [2] L.B. da Silva, J.E. Trebes, R. Balhron, S. Mrowka et al., *Science* 258 (1992) 269.
- [3] L.B. da Silva, T.W. Barbee Jr., J.A. Koch, R.A. London, B.J. MacGowan, D.L. Matthews, D. Minyard, G. Stone, T. Yorkey, E. Anderson, D.T. Attwood, D. Kern, *Opt. Lett.* 17 (1992) 754.
- [4] D.S. Durfee, J.W. Moody, K.D. Brady, C. Brown, B. Campbell, M.K. Durfee, D. Early, E. Hansen, D.W. Madsen, D.B. Morey, P.W.A. Roming, M.B. Savage, P.F. Eastman, V. Jensen, *J. X-ray Sci. Technol.* 5 (1995) 20.
- [5] J.B. Kortright, J.H. Underwood, *Proc. SPIE* 1343 (1990) 95.
- [6] J.E. Byorkholm, J. Bokor, L. Eichner, R.R. Freeman, J. Gregus, T.E. Jewell, W.M. Mansfield, A.A. Mac Dowell, E.L. Raab, W.T. Silfvast, L.H. Szeto, D.M. Tennant, W.K. Waskiewicz, D.L. White, D.L. Windt, O.R. Wood II, J.H. Bruning, *J. Vac. Sci. Technol. B* 8 (1990) 1509.
- [7] J.B. Kortright, M. Rice, K.D. Franck, *Rev. Sci. Instr.* 66 (1995) 1567.
- [8] A.D. Akhsakhalyan, S.V. Gaponov, S.A. Gusev, V.I. Luchin, Yu.Ya. Platonov, N. Salashchenko, *Sov. Phys. Tech. Phys.* 29 (1984) 446.
- [9] S.V. Gavono, A.Ya. Grudskii, S.A. Gusev, Yu.Ya. Platonov, N. Salashchenko, *Sov. Phys. Tech. Phys.* 30 (1985) 339.
- [10] S.V. Gavonov, S.A. Gusev, Yu.Ya. Platonov, N.A. Polushkin, N.N. Salashchenko, N.I. Fomina, A. Fraerman, *Sov. Phys. Tech. Phys.* 32 (1986) 541.
- [11] H. Mai, W. Pompe, *Appl. Surf. Sci.* 54 (1992) 215.
- [12] D. Kim, H.W. Lee, J.J. Lee, J.H. Je, M. Sakurai, M. Watanabe, *J. Vac. Soc. Technol. A* 12 (1994) 148.
- [13] J.H. Underwood, T.W. Barbee, *Appl. Opt.* 20 (1981) 3027.
- [14] D.-E. Kim, D.-H. Cha, *J. Korean Phys. Soc.* 29 (1996) 74.
- [15] D.-E. Kim, D.-H. Cha, S.-W. Lee, *J. Vac. Soc. Technol. A*, Aug. 1997 (in press).
- [16] C. Montcalm, B.T. Sullivan, H. Pepin, J.A. Dobrowolski, M. Sutton, *Appl. Opt.* 33 (1994) 2057.
- [17] S. Nakayama, M. Yanagihara, M. Yamamoto, H. Kimura, T. Namioka, *Phys. Scr.* 41 (1990) 754.